

# Battery Key Performance Projections based on Historical Trends and Chemistries

Blake Tiede, Cody O'Meara, Ralph Jansen

NASA Glenn Research Center

blake.a.tiede@nasa.gov, cody.a.omeara@nasa.gov, ralph.h.jansen@nasa.gov

Recent improvements in state-of-the-art (SOA) batteries driven by the automotive sector have led to many electrified aircraft concepts choosing batteries as the preferred energy-storage method. Current SOA batteries are at the point of enabling certain hybrid and all-electric aircraft, particularly small, short range, lower speed aircraft. Higher performance batteries improve aircraft range and can enable larger, higher speed aircraft. In this work, we develop specific energy projections for future electrified aircraft. The projections are developed based on examining historical commercial SOA trends as well as practical limitations of future chemistries. Accurate projections of future specific energy values are important for estimating the timeline for commercial introduction of electrified aircraft. This work estimates nominal cell level specific energies for rechargeable batteries of 489 Wh/kg by 2030, 638 Wh/kg by 2040, and 764 Wh/kg by 2050. More conservative as well as more aggressive estimates are also provided.

## I. INTRODUCTION

Electrified Aircraft Propulsion (EAP) includes fully electric, hybrid electric, and turboelectric approaches to provide power to electric motors which drive propulsors (fans or propellers) to create thrust. EAP is being considered for the range of aircraft from small drones to 300 passenger future aircraft concepts. Smaller, short range, relatively slowly flying aircraft have already been created with existing battery technologies. Future aircraft battery requirements are highly dependent on mission design and EAP configuration. However, lighter weight and higher efficiency batteries enable certain configurations and increase the benefits for systems that already come close with existing batteries. Misra provides an overview of battery specific energy needs for future aircraft calling out ranges between 250 to 1000 Wh/kg [1] (watt-hour per kilogram). A representative aircraft concept study by Dean examines aircraft performance over ranges between 200 and 1500 Wh/kg [2]. This paper provides an initial projection of future battery specific energy performance based on historical rates of progress and maximum specific energy limits for some select chemistries.

## II. HISTORICAL BATTERY SPECIFIC ENERGY TRENDS

Only secondary batteries were considered in this study. These batteries are rechargeable and would be preferably implemented in Hybrid Electric aircraft to meet emissions targets. Improving battery specific energy density is critical for enabling hybrid electric and all electric aircraft. Specific energy density is defined by the units of watt-hour per kilogram. This is a gravimetric, or weight-focused analysis.

### A. Methodology

Battery data was collected and organized. This battery data includes past and presently available cells and batteries across a wide range of chemistries. Data collected includes release year, specific energy, nominal voltage, C-rate, model level, and availability type. Availability was used to categorize cells and commercially available or only produced for research. Model level identified if the data described cell or pack level properties. Historical cell information was used to create projections of future cell performance. In cases where data was available for both cells and packs with the same chemistry, the knockdown factor (or packing factor) between the cell and battery pack could be determined. Candidate cells were screened to find the most applicable types for Electrified Aircraft Propulsion (EAP) applications. Screened cells have a few key qualities including: cell specific energy sufficient to scale to aircraft batteries, a C-rate greater than or equal to 3C, the best performance of the chemistry and timeframe, and secondary (rechargeable) capabilities.

First, a number of linear and exponential trend projections are made by grouping together subsets of the historical cell data. Performance based groupings were: highest energy density cell every decade, best commercial cell available, and best overall cell (including the most feasible prototype) available. Trends were also generated using chemistry and chemistry technology groupings (such as Li-ion).

The second step was the creation of future performance projections using a Boltzmann Sigmoid, or S-Curve, projection of the agglomerated specific energies data sets. S-Curves have four major variables that equate to right-hand asymptote, left-hand asymptote, inflection point, and a rate of change variable. This process yielded the Boltzmann variables that allowed us to create the S-Curves. S-Curve projections were selected to reflect an initial phase of gradual performance improvement, an intermediary phase of rapid advancement, and a final phase of technology maturation with slowing performance gains.

The available cell performance data set is unevenly distributed by time and chemistry. Data sets were conditioned prior to creation of the S-Curves in order to avoid biases caused by the quantity of data available by decade or chemistry. The projection fits were done by optimizing  $R^2$  over historical trends and data sets by changing the four Boltzmann Sigmoid variables.

## B. Cell and Pack Historical Data

After screening the cells down to potentially viable candidates, the next step is to select the data to be used for the initial linear and exponential trends, along with the S-curve projections. This entailed gathering cell and pack data from a variety of resources. The majority of data came from two databases, A2MAC1 [3] for automotive and Batteriesdatabase.com [4] for commercial-off-the-shelf (COTS) which included a large variety of cells and battery manufactures. Data points were also gathered from a variety of non-COTS sources including and not limited to: Solid Power, Advano, Pipistrel, Tesla, Porsche, Handbook of Batteries [5], NASA, U.S. Department of Energy, Oxis Energy, NexTech, and Rolls Battery. These non-COTS sources provided historic examples and near future prototypes that were not present in the previously mentioned databases. The data was screened using the criteria established in the methodology section and sorted into cell and pack level performance information.

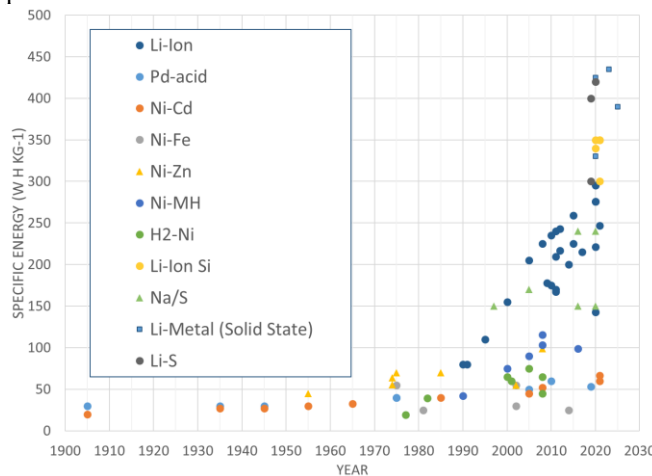


Figure 1. Cell and pack Level Specific Energy Data used in this study organized by chemistry.

## C. Projections using Linear or Exponential Curves

Linear and exponential projection curves were made for subsets of the cell level energy density data. An exponential curve was fitted based on the best performing cell from 1950-2020, excluding Li-S and Li-Metal cells due to their low volume production. With the introduction of Li-ion starting in the 1990s, energy densities rapidly increased. Thus, two linear fits were plotted based on Li-ion cells: one including Si anodes while excluding Li-metal anodes, and another including Li-metal anodes. Each trend and projection were generated without consideration for the density of the data.

The decade-based projection is blind to the different types of chemistry and follow a projection where the highest cell available in each decade is considered in a single data point at the end of the decade. The decade projection starts in 1950 and end in 2020. The year 2020 was decided as a stopping point due to the 2020s being the current decade as of writing. The trend line excludes Li-S and Li-Metal cells due to their extremely low production volumes by 2020.

For the linear trends, a year frequency of every three years was chosen and the max data point available for the chosen condition was provided at that frequency. This prevented higher density data point areas from dominating the trends. An

example of this is the cluster of maximum data points seen in Figure 1 after 2010 in the ~240Wh/kg range.

## D. Discussion of Linear and Exponential Fits

Table I contains the equations and  $R^2$  values of the associated fits seen in Figure 2. The projections in Figure 2 follow the more recent trends in secondary cell technology. The sharp increase in cell-level specific energy is largely driven by advancements in Li-ion technology, including the introduction of Si and Li-metal as anodes. Li-S has also made some advancements, but is a relatively new technology and is not quite ready for large-scale commercial production required for EAP.

Table I. CURVE FIT EQUATIONS AND  $R^2$  VALUES

	Type	Equation	$R^2$
1950-2020 Best Performance	Exp	$y = 1.922 * 10^{-22} * e^{0.0344x}$	0.956
1990-2020 Li-ion + Si	Linear	$y = 8.4692x - 16794$	0.944
1990-2020 Li-ion + Li-Metal	Linear	$y = 9.6056x - 19065$	0.872

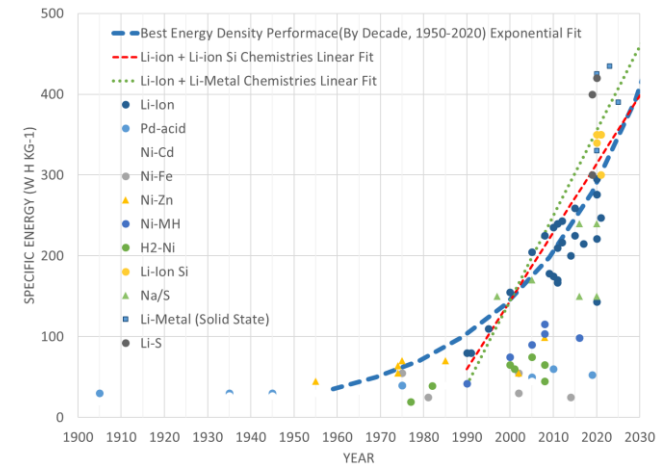


Figure 2. Battery cell energy density historical data, linear, curve fits.

Fitting the exponential curve to the data of the highest specific energy cell from each decade leads to an  $R^2$  value of 0.956, which indicates that the data fits the regression model well. However, as Li-ion technology improves in the 2000s, we can begin to see our exponential curve start to underfit the data, which it continues to do in the present day with the introduction of Si and Li metal anodes. This leads us into examining our two linear fits.

Our linear fits begin with the introduction of Li-ion cells around 1990 and continue into the present day. Over the last 30+ years, Li-ion has been a leader in specific energy and continues to improve due to advancements in cathode, anode, and electrolyte technologies. In pursuit of continuous improvements in specific energy, much focus has been directed on anode materials for Li-ion cells beyond the typical carbon-based anode. Si and Li-metal are two strong candidates due to their high theoretical specific energy.

The first linear fit includes Si in the anode. Si has begun to be used as a dopant in anodes as a means of increasing the specific energy. Cells with pure Si anodes have had trouble reaching the market due to their poor lifetime characteristics,

although there are efforts aimed at pure Si anodes. The linear fit for Li-ion + Si ignores Li-metal and Li-S data due to its low scale production. For the Li-ion + Si linear fit, we have an  $R^2$  value of 0.944.

While Si has been slowly introduced to carbon-based anodes over time, Li metal cells require replacing the entire anode with Li metal. Li metal suffers from safety issues due to the ability to grow dendrites, which can puncture the separator and lead to a short circuit. Multiple companies have been examining how to introduce Li metal as an anode, including using solid state separators or non-flammable electrolytes paired with a passivating layer on the Li metal surface. These technologies have begun to be introduced in pre-commercial products, resulting in cells that have specific energies  $>400$  Wh/kg. While the production is not yet at the level needed to support EAP, it is expected that several companies will be able to increase their production to meet EAP needs within the decade. Because of this, a separate linear fit was used for Li-metal cells due to the drastic increase in specific energy compared to carbon based and/or Si based anodes. Our linear fit of Li-ion + Li-metal has an  $R^2$  value of 0.844. This can be explained by the more drastic increase in specific energy seen by replacing carbon-based anodes with pure Li-metal.

#### E. Cell Level Limits

Each cell has a theoretical limit based on the chemistry of the cathode and the anode. There is also a practical limit, which includes the mass of electrochemically inactive components such as current collectors, separators, electrolyte, additives, tabs, and packaging. A percentage of the theoretical limit can give an insight into how mature a chemistry is, or how close to maturity a chemistry may be. Lithium-ion is difficult to measure maturity due to the mixture of different cathode and anode chemistries.

Theoretical limits of different chemistries were obtained from the work of Zu and Li [6] and presented in Table II. Various cathode and anode pairings were investigated, with the highest theoretical capacity being a sulfur cathode paired with a Lithium-metal anode. For this study, metal-air and metal-oxygen systems were not considered due to the low number of commercial products available as well as the added complexity associated with the balance of plant. Practical limits were estimated by incorporating the mass of the current collectors, assuming an electrolyte-to-sulfur ratio of one, assuming no excess Li (Lithium) metal in the anode, and using practical loading values used in Li-ion electrodes today, estimated using the A2Mac1 benchmarking reports for various cells used in EVs. For the given calculation, the max Li-ion specific energy from Power Sources Database [4] was used. Lithium-Sulfur has large potential by this measure due to high theoretical limit and low realized specific energy.

Table II. BATTERY SPECIFIC ENERGY CHEMISTRY LIMITS

Chemistry	Theoretical Limit (Wh/kg) [6]	Achieved as of 2022 (Wh/kg)	Achieved/Theoretical
LiCoO <sub>2</sub> /C <sub>6</sub>	568	275	48.4%
Pd-Acid	171	55	32.2%
NiMH	240	116	48.3%
Li-S	2654	420	15.8%
Na-S	792	240	30.3%

#### F. Boltzmann Sigmoid Projected Cell Specific Energy

Due to the theoretical and practical limits of specific energy that cells can achieve, eventually exponential and linear fits would exceed the possible specific energy. Because of this, fitting an S-Curve is necessary to provide a more realistic projection than an assumption of continuous, never-ending exponential or linear growth. For this work, a Boltzmann Sigmoid function was used. The Boltzmann Sigmoid function is as follows:

$$S(t) = a + \frac{b}{1 + e^{c(\tau-t)}} \quad (1)$$

where “a” is the left-hand (past) limit, “b” is the right-hand (future) limit, “c” is the S-Curve rate of change, “ $\tau$ ” is the year we achieve half of our theoretical limit, and “t” is the year. The Boltzmann Sigmoid variables were optimized to maximize  $R^2$  of the function to the past data

Past data trends were used to pick out a conservative, nominal, and aggressive trend. The conservative projection is fit to the data from all cells from 1950 to 2010. The nominal projection follows the best in production batteries in the 1990 to 2022 timeframe (which includes recent rapid advances due to competition in the Li-ion space). The optimistic projection includes the best in production batteries in the nominal and advanced prototypes (such as Li-metal and Li-S) that have proven feasibility but are still in the prototype stage.

The conservative and aggressive S-curve projections were built off the historical data selected for each. The fitted S-curve data were sampled at the three-year rate for the aggressive trend and a ten-year rate for the conservative trend. The conservative trend follows improvements every decade over changing chemistries. Like the nominal projection, these trends had an S-Curve fitted to them by maximizing the  $R^2$  value over the trend points.

The final Boltzmann Sigmoid variables for this projection give the continuous function of each projection. The variables are presented in Table III. Through these variables, different aspects of the sigmoid function can be examined. The variable tau ( $\tau$ ) represents the inflection point of the data. This is the point at which the data transitions from rapidly increasing growth to diminishing as the technology matures. This point will be an important test in the future whether technology progression is on track with the projected target.

Table III. CELL ENERGY DENSITY BOLTZMANN VARIABLES

C = Conservative N = Nominal A = Aggressive	Boltzmann Variables		
	C	N	A
a	9.6	0.0	32.5
b	659.1	801.8	1009.0
c	0.0436	0.0607	0.0786
$\tau$	2042.5	2030.8	2030.6

Comparing the projections can be done by examining the Boltzmann variables. The aggressive and nominal projections have similar tau values suggesting that the technology maturation over time may have similar progression pacing, but different asymptote projections. This also lends to the similarity of the two projections. Each of these projections is based more heavily on recent technological progressions. The nominal and aggressive projections are influenced heavily by

the recent developments in Li-ion technology and proposed future developments in Si and Li-metal anodes as well as Li-S cells. Tau for the conservative projection is a later year, representing the more conservative projection will have a longer time before specific energy density increases start diminishing. The three curves can be seen in Figure 4.

#### G. Accuracy of Boltzmann Sigmoid Fits

The S-curve projections were able to fit the underlying data cell specific energy well. S-Curves have approximate  $R^2$  values of 0.94, 0.96, and 0.96 for conservative, nominal, and aggressive projections when compared to the underlying trends. Features in the data can attribute to the high  $R^2$ . However, this high value contributes to a statement of projection accuracy. Projection forecast accuracy then falls on the quality of the data gathered, and the predictability of the conclusions drawn in the entire process.

The nominal S-Curve projection displayed in Figure 3 provides a direct comparison of the S-Curve correlation to the underlying data. This generated an S-Curve that can visibly be seen to match the underlying data well. The projection has a high  $R^2$  value of  $>0.96$  and is calculated using

$$R^2 = \frac{\sum((y_i - f(x_i))^2)}{\sum(y_i - \bar{f})^2} \quad (2)$$

which is the Boltzmann sigmoid error function. Where,  $\bar{f}$  is the mean of the data,  $y_i$  represents the value of the sigmoid in a certain year, and  $f(x_i)$  represents the value of a data point in a certain year. The data is also ‘smoothed’ by only including data points at a specific interval. For data used in the nominal projection, the interval is every three years. This data smoothing allows for data density to not affect the projection and error. However, it does reduce the number of data points that can be used to make the S-Curve projection. It is beneficial to smooth the data this way so the projection stays unbiased to the number of underlying data points over time. The Nominal projection here compares to the raw data points in the “Top Available Production” cell grouping.

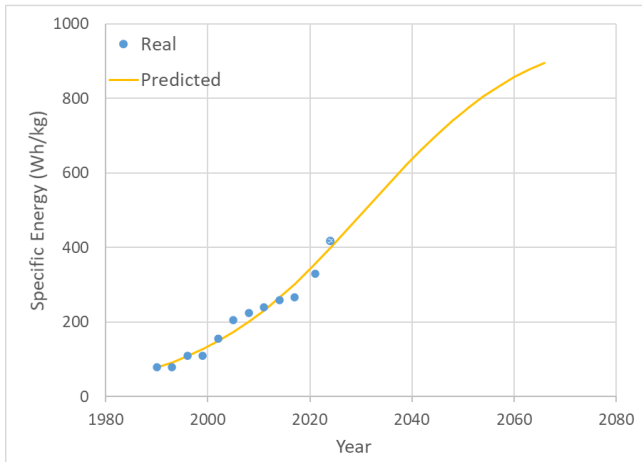


Figure 3. Example S-Curve matching to underlying data. This is the Nominal S-Curve projection and underlying data before the packing factor, or pack knockdown factor, is applied. The projection has an  $R^2$  value of 0.96.

### III. BATTERY LEVEL INFORMATION

#### A. Cell to Pack Derating Factor

While this work reports cell-level specific energies, the true interest to integrators is the pack-level specific energy. To make a functional battery pack, other components besides the cells are needed, including wiring, battery management systems (BMS), thermal management, safety features, and a battery enclosure, among other components. The pack burden, which accounts for the additional components needed to make a functional pack, is heavily dependent on the exact cell chosen and is dependent on many factors, including the form factor, desired safety level in case of thermal runaway, and overall performance of the pack.

Considerable information is available on pack burdens in commercial electric vehicles for a variety of form factors. Information gathered from the A2Mac1 Automotive Benchmarking reports [3] shows that the state-of-the-art (SOA) packing factor is ~60% for soft-case pouch cells, ~70% for cylindrical cells, and has achieved 84.5% for hard-case prismatic cells with the BYD Blade battery design [7-8]. These percentages represent the cell weight percentage of the entire pack. The remaining percentage is accounted for in the wiring, BMS, thermal management systems, safety features, and battery enclosure. Future improvements in the pack burden are expected as cell level technology becomes safer using non-flammable electrolytes and the introduction of solid-state designs. The examples from these sources led 0.7, 0.8, and 0.9 to be the packing factor multipliers to apply to the conservative, nominal, and aggressive. These multipliers would predict packing factor improvement while staying relatively realistic in reference to the prismatic cell BYD Blade battery design. Pack level specific energy S-curve projections were created by multiplying the conservative cell S-curve projection by the conservative packing factor multiplier, the nominal cell S-curve projection by the nominal packing factor multiplier, and the aggressive cell S-curve projection by the aggressive packing factor multiplier. These values can be seen in Table IV.

#### B. Cell to Pack Derating Factor

Li-ion cells are known for their high energy efficiencies, which can approach 100% if discharged at a low enough rate ( $<<C/10$ ). However, practical applications require higher discharge rates, resulting in lower efficiency. Overall efficiency is dependent on factors such as chemistry, cell form factor, electrode structure, and discharge rate.

Real data is used to estimate the efficiency of batteries in practical applications. NASA internal testing data has shown that a commercial 18650 cell designed for high power has an energy efficiency of 95% when discharged at a constant 3C rate. Real-world fast charging data of a 2021 Porsche Taycan has shown the ability to charge from 0% to 100% SOC with 90% efficiency [9]. A 90% charging efficiency and a 95% discharging efficiency lead to a total round trip efficiency, or how much usable energy is available from the energy output from the charger, of 86%, which is used as the conservative estimates for 2030 [10].

Future increases in the efficiency are estimated based on further improvements in the reduction of internal resistance at the cell level and improvements in charging efficiency. These

may come from a variety of factors, including form factor improvements, cell additive improvements, and power management and distribution efficiency improvements. It should be noted that efficiencies will decrease as a function of temperature and cell age. While these estimates are based on real-world conditions, they are mostly made using fresh cells. So, it is expected for the overall efficiency to decrease over the lifetime of the pack. Estimated round-trip efficiencies can be found in Table IV.

#### IV. BATTERY KEY PERFORMANCE PARAMETER PROJECTIONS

Table IV presents the cell and battery level energy densities and the efficiency projections for 2030, 2040, and 2050. Conservative, nominal, and aggressive rates of technology advancement are shown to capture the uncertainty of projecting future progress.

The rate of change in each projection can be seen in Figure 4. The conservative projection is still increasing even after 2050 and is only 85% of its right-hand limit value. This is opposed to the aggressive projection which has reached 95% of its projected right-hand future limit value.

While it is difficult to predict future battery trends and chemistry mixes, these the projected value fall within the limits of the chemistries considered. New chemistries will also enable further advances. For example Li-S has a theoretical specific energy of a Li-S cell is 2,654 Wh/kg. If a Li-S cell is able to achieve ~50% of its theoretical specific energy, which is what LiCoO<sub>2</sub>/C<sub>6</sub> and NiMH cells are able to achieve, then we could see cells with ~1,330 Wh/kg. Metal air chemistries are another potential path to improvement.

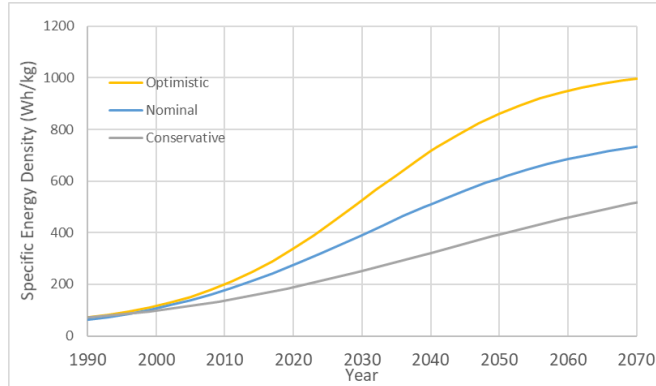


Figure 4. Battery Specific Energy future projections as decided by looking at different

Table IV. BATTERY KEY PERFORMANCE PROJECTIONS

C = Conservative N = Nominal A = Aggressive	2030			2040			2050		
	C	N	A	C	N	A	C	N	A
Cell Level Specific Energy [Wh/kg]	359	489	584	459	638	795	561	764	957
Pack Level Specific Energy [Wh/kg]	251	391	525	321	510	715	393	611	861
Round Trip Efficiency %	86%	89%	92%	87%	90%	93%	88%	91%	94%

#### V. CONCLUSIONS

This paper attempts to project future battery performance based on examining historical commercial SOA trends as well as practical limitations of future chemistries. An S-curve projection of cell energy densities was combined with a packing factor multiplier to project battery pack level specific energies in 2030, 2040, and 2050. This work estimates nominal cell level specific energies for rechargeable batteries of 489 Wh/kg by 2030, 638 Wh/kg by 2040, and 764 Wh/kg by 2050. Efficiency projections provided a basic guide to show gradual progress from the current state of the art toward a four-times reduction in losses by 2050. This work is intended to support aircraft level conceptual modeling of Electrified Aircraft Propulsion (EAP) concepts.

## REFERENCES

- [1] A. Misra, "Energy Storage for Electrified Aircraft: The Need for Better Batteries, Fuel Cells, and Supercapacitors," in IEEE Electrification Magazine, vol. 6, no. 3, pp. 54-61, Sept. 2018, doi: 10.1109/MELE.2018.2849922.
- [2] Mission "Analysis and Component-Level Sensitivity Study of Hybrid-Electric General-Aviation Propulsion Systems," Journal of Aircraft, Vol. 55, No. 6, November–December 2018, doi: 10.2514/1.C034635.
- [3] "A2MAC1 - automotive benchmarking," A2Mac1, 09-Aug-2021.
- [Online]. Available: <https://portal.a2mac1.com/>. [Accessed: 24-Nov-2021].
- [4] Batteriesdatabase.com. [Online]. Available: <http://www.batteriesdatabase.com/App/>. [Accessed: 24-Nov-2021].
- [5] D. Linden and T. B. Reddy, *Handbook of Batteries, third edition*. 2002.
- [6] C.-X. Zu and H. Li, "Thermodynamic analysis on energy densities of batteries," Energy & Environmental Science, vol. 4, no. 8, p. 2614, 2011.
- [7] "BYD Blade prismatic battery cell specs and possibilities (update) - PushEVs." <https://pushevs.com/2020/05/26/byd-blade-prismatic-battery-cell-specs-possibilities/> (accessed Apr. 05, 2022),.
- [8] "Here's Why The Battery Pack of Tesla Model S Plaid is An Electrification Masterpiece - FutureCar.com - via @FutureCar\_Media." <https://www.futurecar.com/5106/Heres-Why-The-Battery-Pack-of-Tesla-Model-S-Plaid-is-An-Electrification-Masterpiece> (accessed Nov. 24, 2021).
- [9] "Lucid Air DC Fast Charge Follow Up: Charging Losses Explained." <https://insideevs.com/news/550923/lucid-air-charging-losses-explained/> (accessed Apr. 06, 2022).
- [10] K. Li and K. J. Tseng, "Energy efficiency of lithium-ion battery used as energy storage devices in micro-grid," IECON 2015 - 41st Annual Conference of the IEEE Industrial Electronics Society, 2015, pp. 005235-005240, doi: 10.1109/IECON.2015.7392923.